

Electronic properties of Cs-based halide perovskites: An *ab-initio* study

Georgia Moschou, Athanasios Koliogiorgos, and Iosif Galanakis*

Department of Materials Science, School of Natural Sciences, University of Patras, GR-26504 Patra, Greece

(Dated: January 23, 2018)

Halide perovskites consist a class of materials under intense investigation due to their potential technological applications like solar cells, optoelectronic devices and catalysis. Recently we have studied using electronic band structure calculations from first principles, the cubic MABX_3 compounds [A. Koliogiorgos et al., Comput. Mater. Sci. **138**, 92 (2017)], where MA stands for the methylammonium cation, B is a divalent cation and X a halogen. We expand our study in the case where Cs stands in place of the MA cation. Our results suggest that the Cs-based compounds exhibit also a variety of lattice constants and energy band gaps. The calculated equilibrium lattice constants differ substantially from the experimental ones. The calculated energy gaps also show large deviations for these lattice constants. Moreover, the use of more sophisticated functionals leads to conflicting changes in the energy gap values and its effect is materials dependent. Our results suggest that contrary to the MA halide perovskites, the Cs halide perovskites consist a more delicate case and there is still a long way for *ab-initio* calculations to accurately describe their structural and electronic properties.

PACS numbers:

INTRODUCTION

Perovskites consist a wide class of materials embracing several hundreds of compounds, since within the same chemical formula a wide range of components can be combined [1, 2]. They were named after the Russian mineralogist Lev Perovski and the name was first used to describe the CaTiO_3 compound [3]. Although several perovskite materials exist in nature [4], the developments in both chemistry and physics of materials led to the growth of novel perovskite materials suitable for several technological applications like solar cells [5], optoelectronics [6] and catalysis [7].

Among perovskites, a very popular subclass are the ones having the chemical formula ABX_3 , where A is a monovalent cation, B a divalent cation and X a halogen atom. Due to the presence of the halogen atom they are widely known as halide perovskites [8]. A wide range of chemical elements can be combined as long as the requirement for charge neutrality is satisfied. Interestingly the A cation can be also a charged organic molecule, e.g. methylammonium, formamidinium etc giving birth to the so-called hybrid or organic-inorganic halide perovskites [2, 8–10]. Among these hybrid halide perovskites special attention has been paid to the methylammonium (MA) based ones [11–15], where the MA cation is CH_3NH_3 , due to the fact that MAPbI_3 has an energy gap of about 1.5–1.7 eV [16, 17] absorbing at the optical regime.

Motivated by the search for lead-free hybrid halide perovskites, in reference [18] we carried out an extended *ab-initio* study of the MABX_3 compounds crystallizing in the cubic structure. As X we considered all possible halogen atoms, namely F, Cl, Br and I. As divalent B cations we took into account the alkali earth elements (Ca, Sr, Ba) since they have two valence p electrons, the late transition metal atoms (Zn, Cd, Hg) which have two

valence s electrons and the metalloids (Ge, Sn, Pb) which have also two valence p electrons but contrary to the alkali earth elements the valence d states are completely occupied. As our results suggested in reference [18] several of these 36 compounds possessed energy gaps within the optical regime, making them suitable for solar cell applications.

In the present study we expand our previous work in the case of the Cs-based compounds having the chemical formula CsBX_3 . First, we considered only the cubic structure, presented in figure 1, taking into account all possible combination of divalent cations and halogen anions as for the MABX_3 compounds mentioned above. For these compounds we computed initially the equilibrium lattice constant and then their electronic properties focusing on the width of the energy band gap. Second, we considered the experimental lattice structures for the CsBX_3 which have been grown successfully and we have calculated the energy band gap also in their case. The latter crystallize not only in the cubic but also in orthorhombic lattices, since as it is well known perovskite materials undergo several structural transitions [8]. The manuscript is organized in the following way. In section we present the details of our calculations. In section we present and discuss our results. Finally, in section we summarize our results and conclude.

COMPUTATIONAL METHOD

The *ab-initio* electronic band structure which has been employed in the present study is the so-called VASP (acronym for Vienna *ab-initio* Simulation Package) developed at the Institut für Metalphysik of the Universität Wien [19]. As pseudopotentials we used the projector augmented waves (PAW) [20]. As exchange correlation

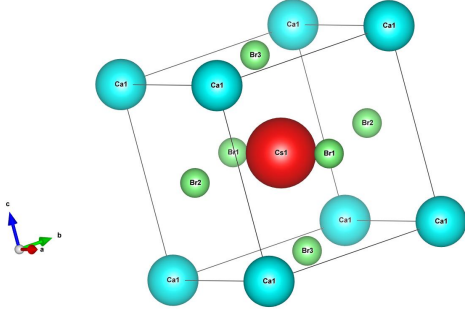


FIG. 1: Schematic representation of the cubic lattice structure assumed for the CsBX_3 compounds. The Cs atom is at the center of the cube, the divalent B cations are at the corners of the cube and the halogen atoms are at the center of the faces.

functional we have used the so-called PBEsol (Perdew-Burke-Ernzerhof for solids) [21, 22], which belongs to the family of the generalized gradient approximation (GGA) functionals. Although GGA functionals in general are known to reproduce accurately the structural properties, they fail to reproduce the energy gap in semiconductors like perovskites although they yield the correct shape of the bands.

Since the exact value of the energy gap is crucial for applications, we have also used in our calculations the modified Becke-Johnson functional in conjunction with the PBEsol one (known as mBJ+PBEsol). The mBJ has been developed in 2006 by Becke and Johnson in an attempt to provide an efficient exchange functional which would reach the accuracy of the hybrid functionals like Heyd-Scuseria-Ernzerhof (HSE06) but which would require CPU resources similar to the GGA calculations [23, 24]. The mBJ functional is a potential-only functional being a local approximation to an atomic exact-exchange potential plus a screening term which is used in conjunction to one of the exchange-correlation schemes (PBEsol in our case). Thus the mBJ-based calculations within VASP are not self-consistent with respect to the total energy [25]. Finally, for the two compounds which have been grown experimentally, CsPbBr_3 and CsPbI_3 , we have also performed calculations using the hybrid HSE06 functional [26], which has been successfully implemented in VASP [27]. HSE06 is well-known to reproduce accurate band gap values for semiconductors but it leads to very demanding calculations, both in cpu time and cpu resources [28]. In the case of the MABX_3 compounds studied in reference [18] both HSE06 and mBJ+PBEsol yielded similar band gap values and thus we expect this to be the case also for the Cs-based compounds. It is worth to notice, that GGA calculations for related ABO_3 perovskites underestimate the band gap value, while the hybrid B3PW and B3LYP functionals allow to achieve much better agreement with the experiment for the band gap values [29, 30].

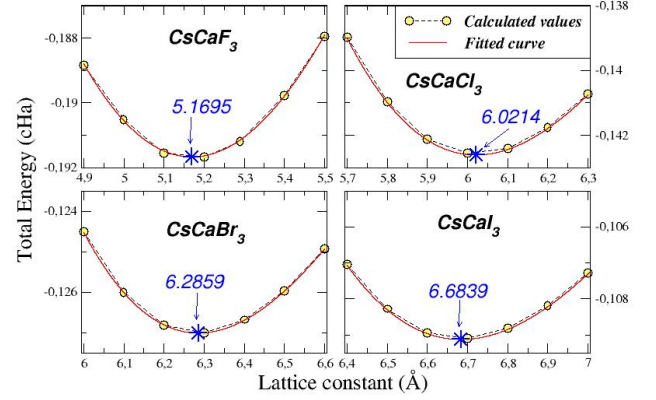


FIG. 2: Calculated total energy versus the lattice constant for the cubic CsCaX_3 compounds. The calculated values have been fitted with a third order polynomial in order to determine the equilibrium lattice constant. Note that the use of the Murnaghan equation of state gives identical results in the case of the compounds under study.

TABLE I: Calculated equilibrium lattice constants, a_{eq} , in Å for the studied cubic halide perovskites using the PBEsol approximation. These perovskites have the chemical formula CsBX_3 where B is a divalent cation and X is a halogen atom.

$a_{eq}^{\text{CsBX}_3}$ (Å)	X=F	X=Cl	X=Br	X=I
B=Ca	5.1695	6.0214	6.2859	6.6839
B=Sr	5.1813	6.0313	6.2947	6.6881
B=Ba	5.1931	6.0452	6.3089	6.7001
B=Zn	5.0125	5.9734	6.3969	7.0772
B=Cd	5.0608	6.0266	6.3710	6.9758
B=Hg	4.9680	5.9715	6.5038	7.1538
B=Ge	5.1153	6.0136	6.3015	6.7670
B=Sn	5.1331	6.0216	6.3020	6.7178
B=Pb	5.1614	6.0274	6.3008	6.7103

Concerning the details of the calculations, we have used for all cubic compounds in the first part of our study, a cutoff for the kinetic energy of the plane waves of 420 eV and for the Ge, Sn and Pb atoms we have included in the PAW basis the $3d$, $4d$ and $5d$ orbitals, respectively, as valence states. For the case of the mBJ+PBEsol calculations we have used a more advanced basis set including also the kinetic energy density of the core electrons. To determine the equilibrium lattice constants we have used a $6 \times 6 \times 6$ Monkhorst-Pack grid in the 1st Brillouin zone [31] in conjunction with the PBEsol functional. For the equilibrium lattice constant, we have used a denser $10 \times 10 \times 10$ grid to calculate the electronic properties. For the compounds adopting the experimental lattice structure we present and discuss the details of the calculations in section and in table III.

RESULTS AND DISCUSSION

Equilibrium lattice constants for the cubic compounds

As mentioned above, we have considered that the compounds under study crystallize in the cubic structure shown in figure 1 [32]. The Cs atoms sit at the center of the cube, the divalent cations sit at the corners of the cube surrounded by halogen atoms in an octahedral environment. To determine the equilibrium lattice constant we have calculated the total energy for seven lattice constant values around the minimum. Then we have fitted a third order polynomial curve to determine the equilibrium lattice constant corresponding to the minimum of the energy. In figure 2 we present the calculated total energy values versus the lattice constant and the fitted curve for the four CsCaX₃ compounds. In all cases the fitting is extremely good passing from all seven calculated points.

In table I, we have gathered the calculated equilibrium lattice constants in Å for all 36 calculated compounds and in figure 3 we have plotted them as a function of the divalent cation to make their behavior clear. The obtained equilibrium lattice constants scan a wide range of values starting from 4.9680 Å in the case of CsHgF₃ up to 7.1538 Å for CsHgI₃. All calculated values are larger than the values for the corresponding MA compounds studied in reference [18] due to the larger atomic radius of Cs compared to the MA cation. In figure 3 it is easier to trace the trends in the equilibrium lattice constants. When the halogen atom is Cl almost all compounds under study have the same lattice constant. In the case of the other three halogens, the compounds where the divalent cation is an alkali earth metal or a metalloid have compa-

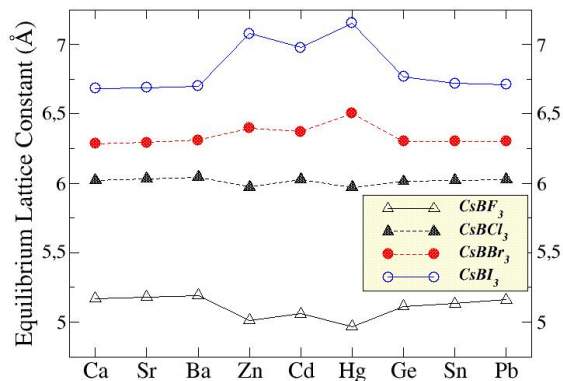


FIG. 3: Behavior of the calculated equilibrium lattice constant for the cubic compounds in Å as a function of the divalent cation. Each line corresponds to a different halogen atom.

TABLE II: Calculated energy gap in eV using the mBJ+PBEsol and PBEsol functionals (the latter in parentheses) for the cubic CsBX₃ halide perovskites and for the equilibrium lattice in table I. The zero values correspond to a gapless (zero-gap) semiconducting behavior. We also provide the HSE06 values in braces where available.

CsBX ₃	X=F	Band gap (eV)		
		mBJ+PBEsol	PBEsol	[HSE06]
B=Ca	1.62(0.59)	0.94(0.58)	0.95(0.41)	0.60(0.24)
B=Sr	2.51(1.40)	1.87(1.10)	1.59(0.79)	1.29(0.64)
B=Ba	3.30(2.14)	2.66(1.88)	2.40(1.50)	1.26(1.26)
B=Zn	0.46(0.00)	0.13(0.00)	0.27(0.00)	0.36(0.00)
B=Cd	0.21(0.00)	0.00(0.00)	0.09(0.00)	0.09(0.00)
B=Hg	0.00(0.00)	0.00(0.00)	0.00(0.00)	0.00(0.00)
B=Ge	0.79(0.00)	0.40(0.00)	0.52(0.00)	0.28(0.00)
B=Sn	0.75(0.00)	0.47(0.00)	0.46(0.00)	0.45(0.00)
B=Pb	0.82(0.00)	0.45(0.00)	0.53(0.00)	[0.49] 0.33(0.00)[0.38]

table values of equilibrium lattice constants. When the divalent cations is one of the three late transition metal atoms, Zn, Cd or Hg, the equilibrium lattice constants show a different behavior and the trend is opposite when the halogen atom is F or I. In the former case the Zn, Cd and Hg based compounds have smaller lattice constant than the other divalent compounds, while in the case of the iodides the Zn, Cd and Hg have considerably larger equilibrium lattice constants with respect to the other divalent cations.

Electronic and gap properties at the theoretical equilibrium lattice constants

Since we have determined the equilibrium lattice constants, we proceeded with the calculation of the energy gaps which is also the main finding of the present study. First, we employed the PBEsol functional. As mentioned above, the former is not accurate enough in most cases to compute the energy gaps, and thus we used the PBEsol calculated electronic charge and wavefunctions as the input to perform electronic band structure calculations with the most accurate mBJ+PBEsol using the same grid in the reciprocal space as for the PBEsol calculations. In table II we have gathered both the mBJ+PBEsol and PBEsol (the latter in parenthesis) calculated energy gaps for all 36 compounds under study. When the divalent cation was a metalloid or a late transition-metal atom, PBEsol led to gapless semiconductors, *i.e.* the gap is vanishing being almost zero. In the case of the alkali earth metals PBEsol produced sizeable gaps ranging from 0.34 eV for CsCaI₃ to 2.14 eV for CsBaF₃.

The use of mBJ+PBEsol opened the gaps in all cases with the exception of the Hg-based compounds. In general the present compounds present very small values of the energy band gaps with respect to the corresponding MA compounds in reference [18]. With few exceptions

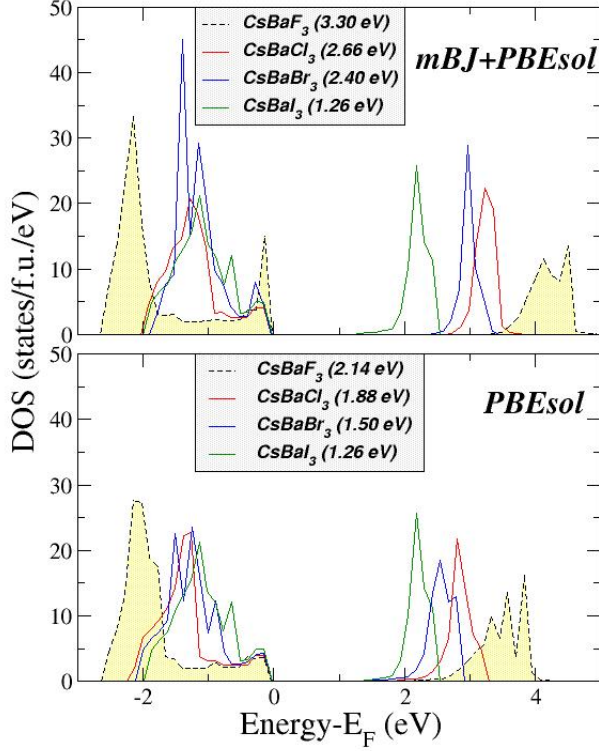


FIG. 4: DOS per formula unit (f.u.) as a function of the energy for the cubic $\text{CsBa}(\text{F, Cl, Br, I})_3$ compounds for the theoretical equilibrium lattice constants using the PBEsol (lower panel) and mBJ+PBEsol (upper panel) functionals. The zero energy corresponds to the Fermi level. Note that the use of the mBJ+PBEsol functional opens the gap but does not influence the character of the bands.

where the gap is almost conserved, the energy band gap becomes smaller as we change the halogen atom going from the light F to the heavy I one. This is expected since the lighter the halogen atom is, the deeper are its valence p states and the larger is the energy gap, *i.e.*, in the case of F the valence states are the $2p$ orbitals while in the case of I the valence states are the $5p$ orbitals which are much higher in energy. Some of the compounds containing alkali earth metals, CsCaF_3 , CsSrCl_3 and CsSrBr_3 have band gaps within the optical regime. In order to elaborate more on the effect of the different functionals, we present in figure 4 the density of states (DOS) for the CsBaX_3 compounds. The mBJ+PBEsol functional, first, shifts the conduction band higher in energy opening the gap with respect to the PBEsol functional. Second, it slightly narrows the bands leading to peaks of larger intensity.

To elucidate the trends observed in the calculated band gap energies, we have plotted in figure 5 the atom- and orbital resolved DOS for the $\text{Cs}(\text{Zn, Ca or Ge})\text{Br}_3$ com-

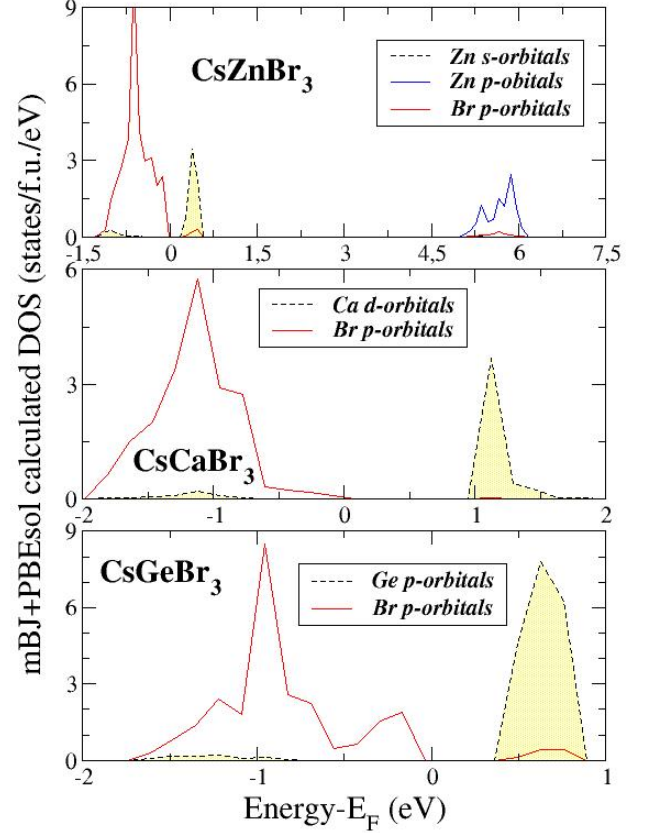


FIG. 5: Atom- and orbital resolved DOS as a function of the energy for the CsZnBr_3 (upper panel), CsCaBr_3 (middle panel) and CsGeBr_3 (lower panel) compounds and for the theoretical equilibrium lattice constant using the mBJ+PBEsol functional. The valence bands for all three compounds consist of the halogen p -orbitals. The conduction bands are made up from the Zn s -, Ca d - and Ge p -states, respectively. The kind of hybridization determines the width of the energy gap.

pounds using the mBJ+PBEsol functional. In all three cases the valence bands are made up from the p states of the Br atoms. Note that in the cubic structure all three Br atoms are equivalent as shown in figure 1. There is also a very small s admixture which is not shown here. In the case of CsGeBr_3 the conduction band is made up from the Ge empty $4p$ states and thus the gap is due to the p - p hybridization; a similar situation occurs if instead of Ge we have the isovalent Sn or Pb. In the case of Ca, and the isovalent Sr and Ba atoms, the conduction band is now made up from the unoccupied triple degenerate t_{2g} d -orbitals which transform in the same way as the p orbitals in the case of tetrahedral and octahedral symmetries. The empty p -states are higher in energy and are not shown in the figure. Finally, when the cation is one of the transition metal atoms (Zn, Cd or Hg), a conduction s -state appears clearly between the occupied p states of

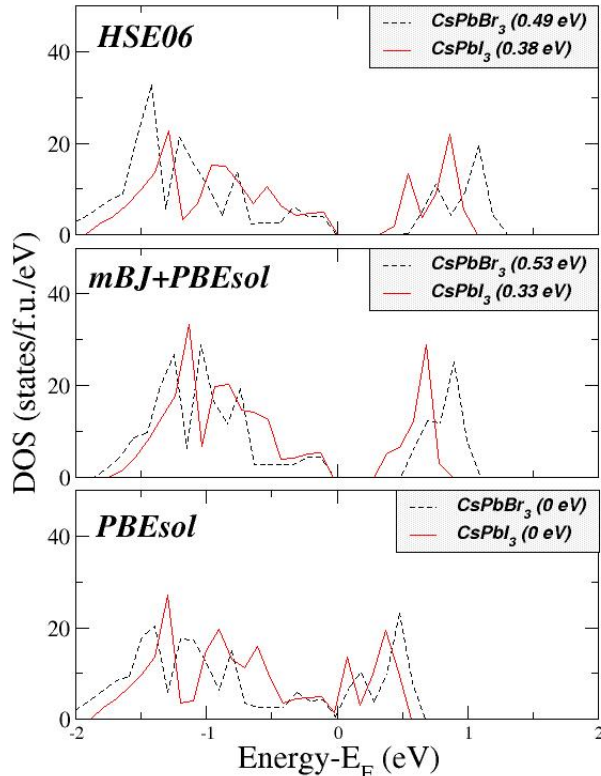


FIG. 6: DOS per f.u. as a function of the energy for the cubic CsPbBr_3 and CsPbI_3 compounds at their theoretical equilibrium lattice constant using the PBEsol (lower panel), mBJ+PBEsol (middle panel) and HSE06 (upper panel) functionals. HSE06 and mBJ+PBEsol open the gap with respect to PBEsol but HSE06 keeps the form of the bands while mBJ+PBEsol leads to narrower bands.

the halogen atoms and the unoccupied p states of the Zn, Cd or Hg atoms. Thus although the p - p hybridization opens a sizeable gap, the location of the Zn, Cd, or Hg s -states within the gap leads to much smaller energy gap values and even to the observed gapless behavior shown in table II.

For the CsPbBr_3 and CsPbI_3 compounds we performed calculations using also the HSE06 functional which is expected to be the state-of-the-art for the computation of energy band gaps in semiconductors to compare it with the mBJ+PBEsol values. HSE06 gave values very close to the mBJ+PBEsol functional; 0.49 eV and 0.38 eV for the CsPbBr_3 and CsPbI_3 compounds, respectively. This behavior is similar to the MA compounds studied in reference [18]. In figure 6 we have plotted for both compounds the DOS using all three PBEsol, mBJ+PBEsol and HSE06 functionals. As can be deduced from the figure HSE06 shifts the conduction bands to higher energy values, similarly to the mBJ+PBEsol functional, but contrary to the latter it does not affect the shape

of the bands.

Electronic properties for the experimental lattice structures

The energy band gaps which were calculated in the above section deviate strongly from the experimentally determined bands gaps for the cubic CsPbI_3 in reference [33]. The theoretical value in table II is 0.33 eV using the mBJ+PBEsol functional while the experimental one is 1.73 eV [33]. A close look in reference [33] reveals that the experimental lattice constant of 6.1769 Å deviates also strongly from the theoretically determined equilibrium lattice constant of 6.7103 Å. Thus one could assume that the discrepancy stems from the difference in the lattice constants. To elucidate more we have carried out *ab-initio* calculations for a series of Cs-based halide perovskites which have been grown experimentally. We have gathered in table III the reference where the compounds have been grown, the details of the lattice structure, the details of the calculations and the calculated band gaps using both PBEsol and mBJ+PBEsol functionals. The lattice of these compounds as determined experimentally are either cubic or orthorhombic. For the orthorhombic the energy cutoff used is 280 eV. The compounds crystallizing in the cubic structure of figure 1 are CsSnCl_3 [34], CsPbCl_3 [35], CsPbBr_3 [36, 37] and CsPbI_3 [33]; note that for CsPbBr_3 there are two different experimental lattice constants of 5.605 Å [36] and 5.870 Å [37]. CsPbF_3 crystallizes also in a cubic structure but now the F atoms are located at the center of the edges and not at the center of the faces [38]. If we compare the experimental lattice constants for the cubic compounds in table III with the theoretical equilibrium lattice constants in table I, we can remark that the deviations are very important; for example for CsSnCl_3 the experimental lattice constant is 5.504 Å and the theoretical one 6.0216 Å. In all cases the experimental lattice constants are about 0.5 Å smaller than the theoretical ones. Thus contrary to the MA-based halide perovskites, in the case of the Cs-based halide perovskites, PBEsol fails to reproduce accurately the lattice constants.

The smaller lattice constants lead also to large deviations in the calculated band gaps. Contrary to the theoretical equilibrium lattice constants, where PBEsol produced gapless behavior for all compounds where the divalent cation was Sn or Pb, in the case of the cubic experimental lattice constants the PBEsol energy band gaps are sizeable and range from 0.97 eV for CsSnCl_3 to 1.72 eV for cubic CsPbBr_3 where the lattice constant is 5.870 Å [37]. Interestingly when the lattice constant of CsPbBr_3 drops to 5.605 Å [36], the energy band gap shrinks to 1.12 eV. The calculated energy band gap for CsPbI_3 using PBEsol is 1.40 eV close to the experimental value of 1.73 eV [33]. The PBEsol calculated band

TABLE III: For the compounds which have been grown experimentally, we present the reference,, the details of the experimental lattice structure, the \mathbf{k} -grid used in the reciprocal space and the calculated energy band gaps in eV using the PBEsol and mBJ+PBEsol functionals.

Compounds	Space group	Lattice	Lattice constants (Å)	\mathbf{k} -point grid	PBEsol (eV)	mBJ+PBEsol (eV)
CsSnCl ₃ [34]	Pm3m	cubic	5.504	10x10x10	0.92	0.97
CsSnI ₃ [41]	Pnma	orthorhombic	10.349x4.763x17.684	4x8x2	1.89	0.96
CsPbF ₃ [38]	Pm3m	cubic	4.475	10x10x10	2.62	3.94
CsPbCl ₃ [35]	Pm3m	cubic	5.605	10x10x10	1.94	2.04
CsPbBr ₃ [36]	Pm3m	cubic	5.605	10x10x10	1.12	0.69
CsPbBr ₃ [37]	Pm3m	cubic	5.870	10x10x10	1.72	0.98
CsPbBr ₃ [40]	Pnma	orthorhombic	8.244x11.735x8.198	6x4x6	1.61	0.78
CsPbBr ₃ [37]	Pbnm	orthorhombic	8.207x8.255x11.759	6x6x4	1.61	0.88
CsPbI ₃ [33]	Pm3m	cubic	6.1769	10x10x10	1.40	0.67
CsPbI ₃ [39]	Pnma	orthorhombic	10.434x4.791x17.761	4x7x2	2.29	1.07

gaps for the orthorhombic structures are slightly larger reaching the 2.29 eV for CsPbI₃ [39]. We can compare our calculated value of 1.61 eV for CsPbBr₃ in the orthorhombic structure with the experimental value of 2.25 eV [40]. We can see that the discrepancy is considerably large. Thus we employed for all compounds under study also the mBJ+PBEsol functional. As discussed in detail in reference [18], mBJ+PBEsol is not guaranteed to open the energy band gaps with respect to PBEsol and its effect is material specific. This is also reflected in our results. There are compounds like CsPbF₃ where mBJ+PBEsol increases the band gap from 2.62 eV to 3.94 eV as was the case for the totality of MA-halide perovskites in reference [18], but in most cases presented in table III mBJ+PBEsol leads to a shrinking of the compounds and cubic CsPbI₃ shows a gap of 0.67 eV and orthorhombic CsPbBr₃ of 0.78 eV deteriorating the agreement between calculations and experiments [33, 40]. We were not able to perform further calculations using the HSE06 functional due to our limitations in computer resources.

SUMMARY AND CONCLUSIONS

Perovskites are materials of particular technological interest due to their versatile applications ranging from solar cells to optoelectronic devices and catalysis. In an attempt to identify halide perovskites, we employed *ab-initio* electronic structure calculations and studied, first, the structural and electronic properties of cubic CsBX₃ compounds with the divalent cation B being one of the Ca, Sr, Ba, Zn, Cd, Hg, Ge, Sn or Pb atoms considering all possible halogen atoms X= F, Cl, Br and I. The first step in our study was to use the VASP *ab-initio* technique in conjunction with the Perdew-Burke-Ernzerhof for solids (PBEsol) functional for the exchange-correlation to determine the equilibrium lattice constants for all 36 compounds. Then for the theoretical equilibrium lattice constant we made use of the more sophisticated mBJ+PBEsol functional and com-

puted the energy band gaps. In most cases usual PBEsol produced gapless semiconductors, but mBJ+PBEsol led to the appearance of energy band gaps.

Since the calculated equilibrium lattice constants differed substantially from the experimental ones (where available), we also carried out electronic structure calculations for several compounds which have been grown experimentally and for which data existed on their lattice structure. These compounds crystallize both in the cubic as well as the orthorhombic structure. The energy gaps calculated with PBEsol were greatly enhanced with respect to the ones at the calculated equilibrium lattice constant. But in most cases the hybrid modified Becke-Johnson (mBJ)+PBEsol functionals led to narrower energy band gaps.

Our calculations suggest that the case of CsBX₃ halide perovskites, unlike other families of halide perovskites, is not trivial and discrepancies between theory and experiments as well as between various functionals occur. Thus further investigation is needed to clarify these points and allow for a more accurate study of these materials in the future.

Acknowledgements

Authors acknowledge financial support from the project PERMASOL (FFG project number: 848929).

* Electronic address: galanakis@upatras.gr

- [1] Q. Chen, N. De Marco, Y. Yang, T. Song, C. Chen, H. Zhao, Z. Hong, H. Zhou, and Y. Yang, *Nano Today* **10**, 355 (2015).
- [2] M. Grätzel, *Nat. Mater.* **13**, 838 (2014).
- [3] M. A. Pena and J. L. G. Fierro, *Chem. Rev.* **101**, 1981 (2001).
- [4] K. Hirose, R. Sinmyo, and J. Hernlund, *Science* **358**, 734 (2017).

- [5] J.-P. Correa-Baena, M. Saliba, T. Buonassisi, M. Grätzel, A. Abate, W. Tress, and A. Hagfeldt, *Science* **358**, 739 (2017).
- [6] M. V. Kovalenko, L. Protesescu, and M. I. Bodnarchuk, *Science* **358**, 745 (2017).
- [7] J. Hwang, R. R. Rao, L. Giordano, Y. Katayama, Y. Yu, and Y. Shao-Horn, *Science* **358**, 751 (2017).
- [8] S. F. Hoefler, G. Trimmel, and T. Rath, *Monatsh. Chem.* **148**, 795 (2017).
- [9] L. Yang, A. T. Barrows, D. G. Lidzey, and T. Wang, *Rep. Prog. Phys.* **79**, 026501 (2016).
- [10] G. C. Papavassiliou, G. Pagona, N. Karousis, G. A. Mousdis, I. Koutselas, and A. Vassilakopoulou, *J. Mat. Chem.* **22**, 8271 (2012).
- [11] S. Brittan, G. W. P. Adhyaksa, and E. C. Garnett, *MRS Commun.* **5**, 7 (2015).
- [12] J. M. Frost, K. T. Butler, F. Brivio, C. H. Hendon, M. van Schilfgaarde, and A. Walsh, *Nano Lett.* **14**, 2584 (2014).
- [13] A. Filippetti, A. Mattoni, *Phys. Rev. B* **89**, 125203 (2014).
- [14] J. Albero, A. M. Asiri, and H. Garcia, *J. Mater. Chem. A* **4**, 4353 (2016).
- [15] Y. Zhou, M. Yang, O. S. Game, W. Wu, J. Kwun, M. A. Strauss, Y. Yan, J. Huang, K. Zhu, and N. P. Padture, *ACS Appl. Mater. Interfaces* **8**, 2232 (2016).
- [16] Y. Zhao and K. Zhu, *Chem. Soc. Rev.* **45**, 655 (2016).
- [17] C. Quarti, E. Mosconi, J. M. Ball, V. DInnocenzo, C. Tao, S. Pathak, H. J. Snaith, A. Petrozza, and F. De Angelis, *Energy Environ. Sci.* **9**, 155 (2016).
- [18] A. Koliogiorgos, S. Baskoutas, and I. Galanakis, *Comput. Mater. Sci.* **138**, 92 (2017).
- [19] G. Kresse and J. Furthmüller, *Phys. Rev. B* **54**, 11169 (1996).
- [20] J. Kresse and D. Joubert, *Phys. Rev. B* **59**, 1758 (1999).
- [21] J. P. Perdew, K. Burke, and M. Ernzerhof, *Phys. Rev. Lett.* **77**, 3865 (1998).
- [22] J. P. Perdew, A. Ruzsinszky, G. I. Csonka, O. A. Vydrov, G. E. Scuseria, L. A. Constantin, X. Zhou, and K. Burke, *Phys. Rev. Lett.* **100**, 136406 (2008); *ibid.* **102**, 039902(E) (2009).
- [23] A. D. Becke and E. R. Johnson, *J. Chem. Phys.* **124**, 221101 (2006).
- [24] F. Tran and P. Blaha, *Phys. Rev. Lett.* **102**, 226401 (2009).
- [25] <https://cms.mpi.univie.ac.at/vasp/vasp/meta.GGAs.html>
- [26] J. Heyd, G. E. Scuseria, and M. Ernzerhof, *J. Chem. Phys.* **118**, 8207 (2003); *ibid.* **124**, 219906(E) (2006).
- [27] J. Paier, M. Marsman, K. Hummer, G. Kresse, I. C. Gerber, and J. G. Ángyán, *J. Chem. Phys.* **124**, 154709 (2006); *ibid.* **125**, 249901(E) (2006).
- [28] C. Franchini, *J. Phys.: Condens. Matter* **26**, 253202 (2016).
- [29] R. I. Eglitis, *Appl. Surf. Sci.* **358**, 556 (2015).
- [30] R. I. Eglitis, *Phys. St. Sol. B* **252**, 635 (2015).
- [31] H. J. Monkhorst and J. D. Pack, *Phys. Rev. B* **13**, 135188 (1976).
- [32] A. M. A. Leguy, J. M. Frost, A. P. McMahon, V. G. Sakai, W. Kockelmann, C. Law, X. Li, F. Foglia, A. Walsh, B. C. O'Regan, J. Nelson, J. T. Cabral, and P. R. F. Barnes, *Nature Commun.* **6**, 7124 (2015).
- [33] G. E. Eperon, G. M. Paterno, R. J. Sutton, A. Zampetti, A. A. Haghighirad, F. Cacialli, and H. J. Snaith, *J. Mater. Chem. A* **3**, 19688 (2015).
- [34] G. G. Bulanov, A. B. Podlesskaya, L. V. Soboleva, and A. I. Soklakov, *Izvestiya Akademii Nauk SSSR, Neorganicheskie Materialy* **8**, 1930 (1972).
- [35] J. Hutton, R. J. Nemes, G. M. Meyer, and V. R. Eiriks-son, *J. Phys. C: Sol. St. Phys* **12**, 5393 (1979).
- [36] M. Sakata, T. Nishiwaki, and J. Harada, *J. Phys. Soc. Japan* **47**, 232 (1979).
- [37] M. Rodová, J. Brozek, K. Knzek, and K. Nitsch, *J. of Thermal Analysis* **71**, 667 (2003).
- [38] P. Berastegui, S. Hull, and S.-G. Eriksson, *J. Phys.: Cond. Mat.* **13**, 5077 (2001).
- [39] C. C. Stoumpos, C. D. Malliakas, and M. G. Kanatzidis, *Inorg. Chem.* **52**, 9019 (2013).
- [40] C. C. Stoumpos, C. D. Malliakas, J. Peters, Z. Liu, M. Sebastian, J. Im, T. C. Chasapis, A. C. Wibowo, D. Y. Chung, A. J. Freeman, B. W. Wessels, and M. G. Kanatzidis, *Cryst. Growth Des.* **13**, 2722 (2013).
- [41] I. Chung, J.-H. Song, J. Im, J. Androulakis, C. D. Malliakas, H. Li, A. J. Freeman, J. T. Kenney, and M. G. Kanatzidis, *J. Amer. Chem. Soc.* **134**, 8579 (2012).